A Radiation Belt MeV Electron Flux Comparison Between RBE and GOES-15

April 10, 2015

Lois Keller Sarno-Smith

Introduction

Earth's radiation belts are two large and distinct toruses of high energy plasma that surround Earth. The highly stable inner belt is composed mostly of relativistic protons and lies approximately 1.2-3 Earth radii away from Earth's surface. The outer belt, located at 4-7 Earth radii away from the surface, is compromised of mostly relativistic and ultra relativistic electrons. The outer belt is highly dynamic and sensitive to changes in geomagnetic activity and the solar wind. Figure 1 shows the radiation belt in context of Earth and geosynchronous orbit. A small distortion in Earth's magnetic field can lead to orders of magnitude changes in electron differential number fluxes.

The high energy electrons of the outer belt also pose a major threat to geosynchronous satellites. Geosynchronous orbit, a popular orbit for communications and defense satellites, lies in the outer radiation belt. Unfortunately, relativistic electrons can penetrate the aluminum shielding on satellites, which can cause circuitry upsets and sometimes generate large internal electric fields on satellites [2]. Cumulative radiation exposure destroys satellites, so considering relativistic electron flux levels is critical for geosynchronous satellite mission planning. Consequently, we need accurate models for predicting relativistic electron flux levels at geosynchronous orbit.

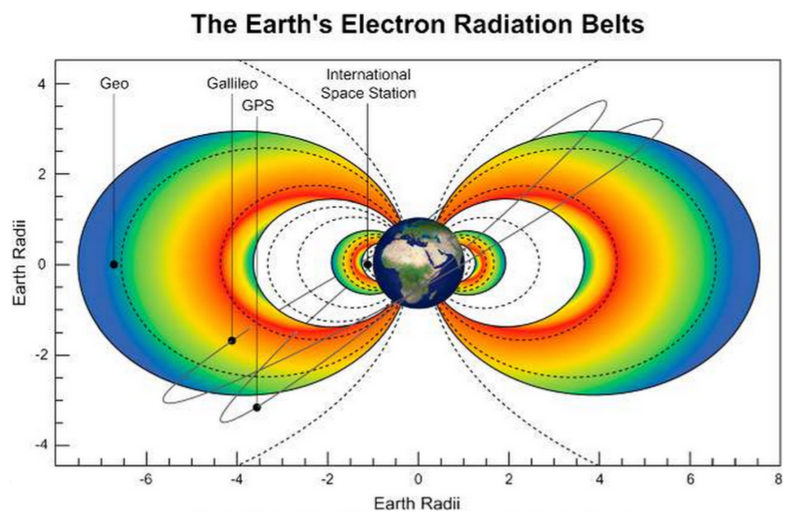

Figure 1: Earth's radiation belts (inner and outer) where color serves as a proxy for flux levels. Telecommunications satellites such as Gailileo and GPS are shown to highlight their position relative to the high energy electron outer belt. Reproduced from [1].

The Radiation Belt Environment (RBE) model is a data driven kinetic model that aims to determine temporal variation in the phase space density of energetic electrons using a version of the bounce averaged Boltzmann transport equation (see [3, 4]). Figure 2 shows how inputs are received and processed in RBE, namely how the solar wind data from ACE is interpreted by the sub-models within RBE. Since RBE is a kinetic model, the particle distribution function is solved numerically. RBE's notable feature is the calculation of electron fluxes via solving the radial diffusion equation driven by the solar wind and using convective transport of ring current particles to higher energies to best capture electron flux levels.

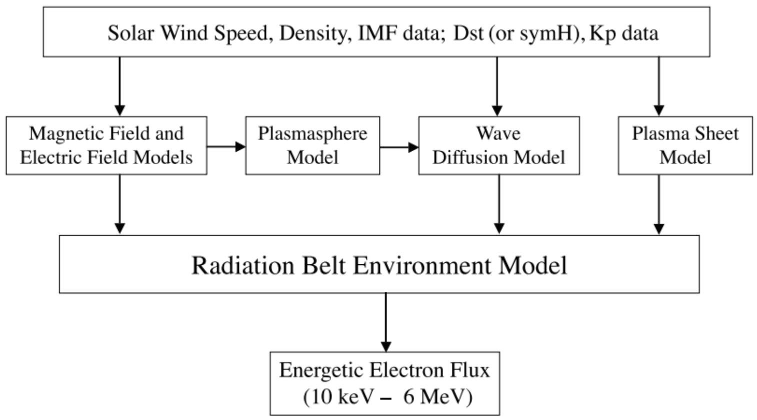

Figure 2: RBE flow chart on models it draws from, reproduced from [3].

RBE also includes wave particle interactions from whistler mode chorus waves. Specifically, RBE incorporates diffusion coefficients from the Pitch Angle and Energy Diffusion of Ions and Electrons (PADIE) code [5]. The bounce averaged drift velocities of the electrons are calculated by including gradient and curvature drift along with E x B drift from convection and corotation electric fields [3]. The wave activity sensitive part of the Boltzmann transport equation depends on the magnetic field conditions, which is key in analyzing how well RBE catches storm time recovery periods and depolarization events.

RBE's inclusion in the Space Weather Modeling Framework (SWMF) and coupling with Ionosphere Electrodynamics (IE), the Rice Convection Model (RCM) and the global magnetosphere effects from the Block-Adaptive-Tree-Solarwind-Roe-Upwind-Scheme (BATSRUS) augments RBE's ability to capture small perturbations and feedbacks [6]. RBE coupled with SWMF is a model available on the Community Coordinated Modeling Center (CCMC) website and results in 2D slice of the radiation belts in the equatorial plane with energy resolution available between 10 keV to 4 MeV. Figure 3 shows the 2 MeV electron fluxes given by RBE during an injection on 2013-05-07 using CCMC's visualization tools.

Another challenge in modeling electron radiation belt populations is in comparing them to data. The high energy electron fluxes are extremely sensitive to changes in magnetic latitude, distance from Earth, and measured/modeled particle energy. Ideally, we would want to compare RBE, an equatorial 2-D model, with a satellite at a fixed radial distance from Earth with zero orbital inclination at identical energies. Although missions like the Van Allen Probes and the Solar, Anomalous, Magnetospheric Particle Explorer (SAMPEX) have the capability to make fantastic MeV electron measurements, the orbital inclinations of these missions (15 and 82 degrees respectively), make it challenging to make a fair comparison to GSM-equatorial plane locked RBE electron fluxes [7, 8]. The Los Alamos National Laboratory Synchronous Orbit Particle Analyzer (LANL SOPA) would be ideal, but the data is only available on a case-by-case basis, and we were unable to acquire this data for the deadline of this study.

However, we are fortunate to have the Geostationary Operational Environment Satellite (GOES) 15. GOES-15 is an geosynchronous satellite launched in 2010 into geosynchronous orbit [9] with little to no orbital inclination. The Electron, Proton, and Alpha Detector (EPEAD) instrument measures high energy electrons in two channels, E1 > 0.8 MeV and E2 > 2 MeV. We use the second channel in our study and make the assumption that the measured fluxes from

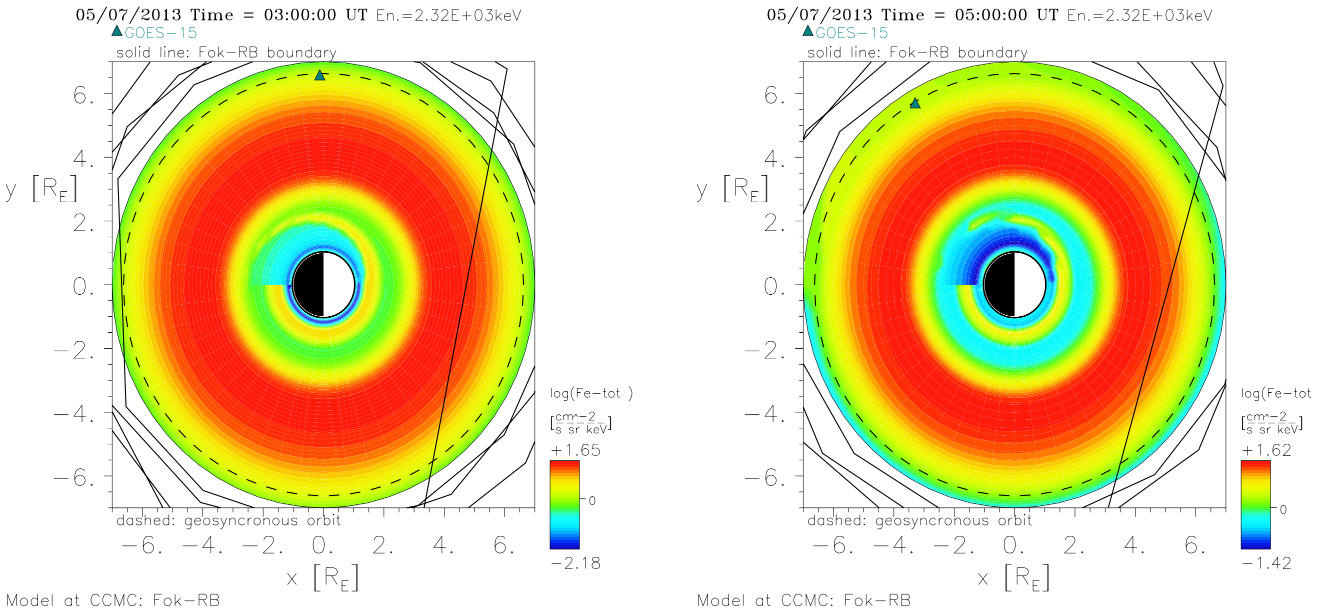

Figure 3: CCMC provided RBE electron fluxes at 2 MeV for 2013-05-07 at 3:00 UT and at 5:00UT. The triangle shows the position of GOES-15 at this time.

GOES-15 should be higher than the 2.3 MeV RBE electron fluxes.

In this study, we focus on comparing RBE 2 MeV electron fluxes with GOES-15 2+ MeV electron fluxes to test RBE's ability to capture radiation belt electron dynamics in a variety of geomagnetic conditions. After overcoming several initial challenges and misconceptions, our project evolved into a comparison study of RBE and GOES-15 on a 10 hour period on an injection day and the following day. We also quantify how long RBE must be run to produce valid results on the days we examine. This report will largely focus on the methods we took to obtain our results, since the fruit of our labor is still forthcoming (in other words, the code is running on CCMC now).

Challenges/Methods

As aforementioned, it is difficult to directly compare RBE output with GOES-15 output, especially since GOES-15 measurements include all particles > 2 MeV. Ideally, we envisioned determining a constant offset between the data and model output during quiet time to account for the anticipated higher fluxes from the > 2 MeV in GOES-15 data. To compare the two data sets, we performed 24 hour runs for 2013-05-07, 2013-05-08, and 2013-05-12 (injection, post-injection, and isolated quiet time respectively) on CCMC for RBE and retrieved the GOES-15 data for these dates from NASA CDAWeb. Later, we also added a 48 hour RBE run from 2015-03-17 to 2015-03-18, where we observe a very intense geomagnetic storm and the radiation belts' initial recovery period. For our CCMC runs, we used BATS-R-US as our global magnetosphere model, version 2014-06-11. For our events in 2013, we used ACE Level 2 data, but for events in 2015 we used ACE-realtime data. Specifically, we had the Fok Ring Current turned off, RCM turned on, CRCM off, auroral conductance on, and recalculation of the polar cap turned on.

However, when we compared the data and model results, we found that RBE fluxes did not exhibit the expected peak at noon typical of the outer belt electron populations due to solar wind magnetospheric compression. Instead, RBE fluxes showed a high peak in electron fluxes at dusk which plummeted across the nightside and dayside. Figure 4 shows the electron fluxes from both RBE and GOES-15 on a quiet day. GOES-15 shows the expected radiation belt electron flux distribution, but RBE behaves strangely, with a peak at dusk and a minimum at noon.

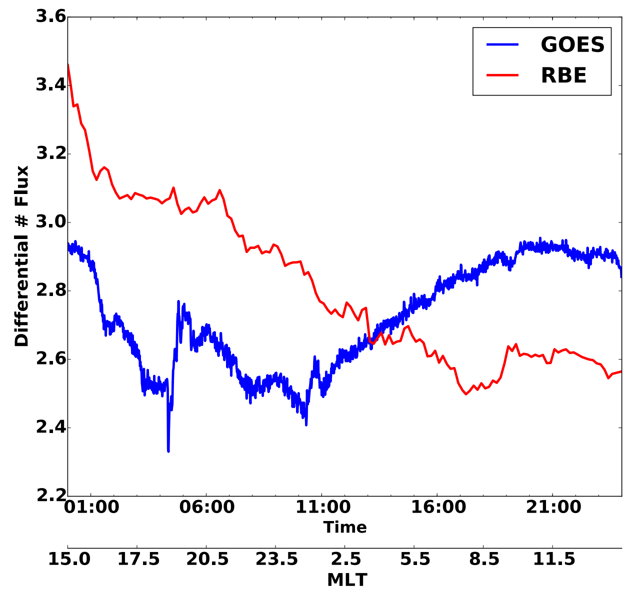

Figure 4: Outer radiation belt electron fluxes for GOES-15 and RBE on 2013-05-12, which was a geomagnetically quiet day.

The electron flux mis-match was due to a constant electron flux loss in RBE at all MLTs across our 24 hour runs. Initially, we thought this was an offset issue and that shifting MLT by 6 hours or so, we would find the model and data align better. Further testing revealed though that the problem was in how RBE's default state as a model was a large injection centered around dawn and uniform fluxes elsewhere. Figure 5 shows the initial state of RBE, regardless of solar wind conditions, which was problematic for our study.

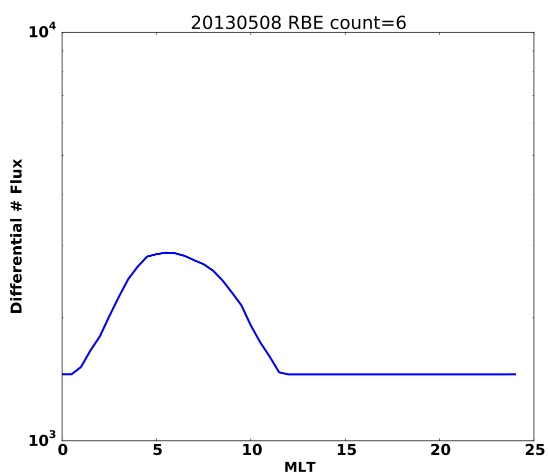

Figure 5: Initial state of RBE on 2013-05-08, with a large injection centered around dawn and uniform fluxes elsewhere.

Our next challenge was then to determine how much time must pass before RBE evolves into a realistic representation of the radiation belts. Figure 6 demonstrates how RBE electron fluxes decrease at all MLTs with increasing time in three of the runs we performed. There is some noise in the runs, especially in (A), which was our injection day (2013-05-07). It is also interesting to note that in (B), beyond approximately 18 UT (orange colored lines), the electron fluxes have a relative peak at MLT=12, which is what the GOES-15 data shows. Further investigation and consultation with the CCMC team revealed that RBE needs ample pre-run time to adjust to the conditions. We determined by examining the electron flux output at each 10 minute interval on 2013-05-07 and 2013-05-08 that approximately 14 hours of pre-run time was enough to give viable electron flux values. However, a day or more of pre-run time would be ideal.

At this point, time constraints limited our analysis to comparing 14 UT to 24 UT on 2013-05-07, 2013-05-08, and 2013-05-12 between RBE and GOES-15. We start by calculating the MLT position of the GOES-15 satellite, which is the time of the flux measurement minus 9 hours since GOES-15 is fixed at 135 degrees W longitude. We then select the the second energy of GOES-15 ('E2') which is the channel that measures all electron fluxes above 2 MeV.

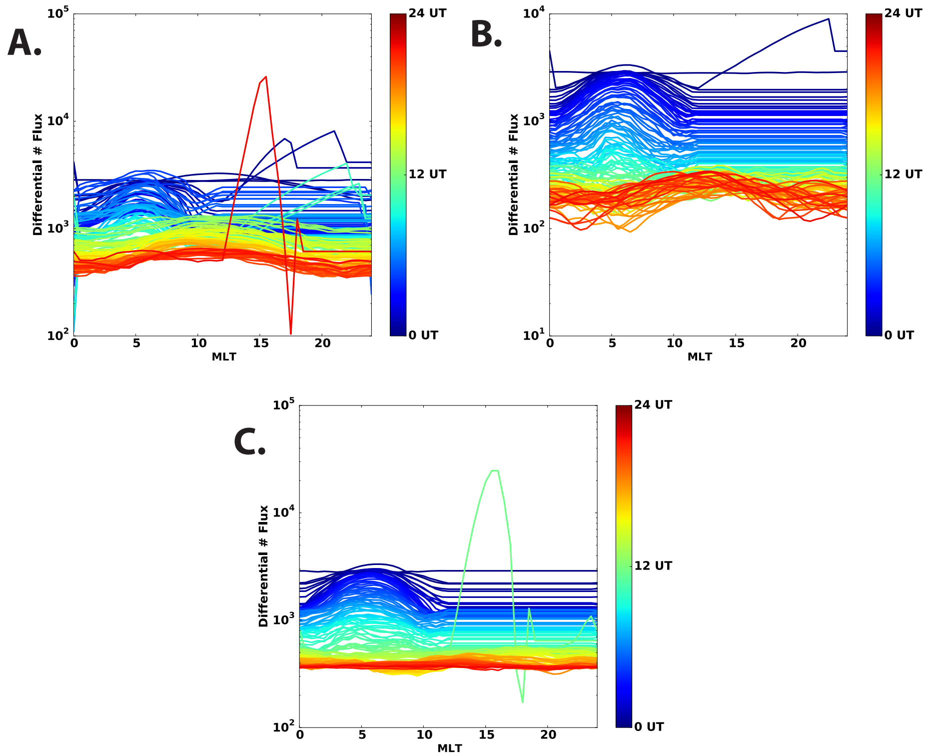

Figure 6: RBE 2.3 MeV electron fluxes across all MLTs on (A) 2013-05-07, (B) 2013-05-08, and (C) 2013-05-12. The color of the line reflects the time in UT of each day, where blue is the beginning of the day (00 UT) and red is the end of the day (24 UT).

Then, we extracted the RBE 2.3 MeV fluxes at the same MLT location as the GOES-15 satellite at each RBE time interval (10 minutes). We then linearly interpolated the RBE data onto GOES-15 satellite time, which created more data points for the RBE to match the number of GOES-15 electron flux measurements. At this point, the GOES-15 electron flux measurements and RBE electron flux outputs are ready for comparison and analysis.

Results

We initially wanted to test RBE's ability to capture radiation belt electron flux changes during injections. Consequently, we chose 2013-05-07 because of the high AE variability throughout the morning and the turning of Bz in the ACE data. Figure 7 shows the AE index on the right and ACE data on the left, provided by CCMC with the 2013-05-07 run. AE index spikes have been associated with substorm injections [10], which is why chose to use 2013-05-07 to test RBE's ability to model injections.

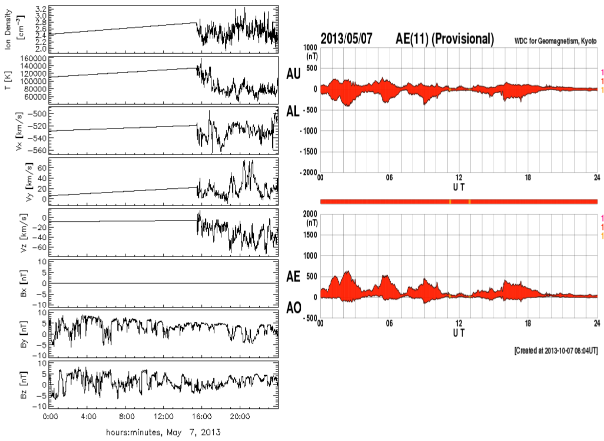

Figure 7: ACE data provided by CCMC for 2013-05-07 on the right along with AE index from Kyoto on the left.

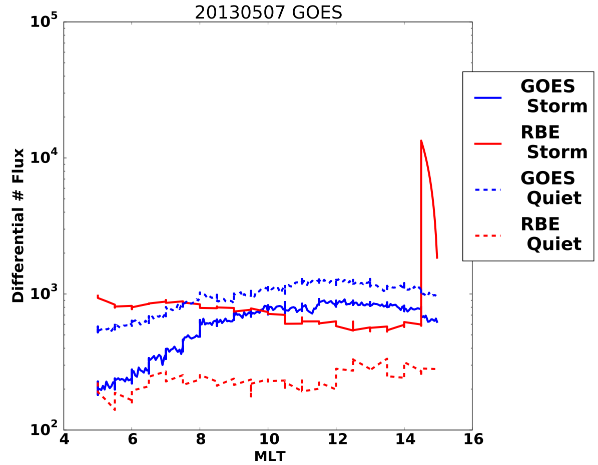

Figure 8: A comparison of GOES-15 2+ MeV electron flux and RBE 2.3 MeV electron flux from 2013-05-07 (storm) and 2013-05-08 (quiet).

Our first direct comparison of the quiet time and injection time results from GOES-15 and RBE is shown in Figure 8. Here, we see that the offset between storm time GOES-15 and quiet time and storm time is minimal, particularly around MLT = 12. The rise of the electron fluxes is similar, with a peak at MLT = 12. The curve is flatter on the quiet day, and the flux values on the quiet day is higher than the flux on the injection day.

On the other hand, Figure 8 shows that RBE fluxes are showing the opposite result. RBE 2.3 MeV electron fluxes are greater on the injection day than on the quiet day by almost an order of magnitude. Also, the expected noon peak is absent in the RBE fluxes. This may still be an artifact of the initial RBE injection not completely dispersing within the time frame of a day. The concerning part of Figure 8 is that RBE does not capture the post-injection rise of MeV electron fluxes, as seen by GOES -15.

Figure 9 shows the electron fluxes from 2013-05-08 (post-injection day) and 2013-05-12 (quiet). We can see that the GOES-15 results from the two quiet periods is very similar, with the post-injection electron fluxes slightly higher than the quiet time ones, especially at MLT = 8 through MLT = 14. Although it is difficult to say from one comparison, it would appear as if there was a rise in electron fluxes during radiation belt recovery which then slowly attenuates over the course of several days from the GOES-15 results.

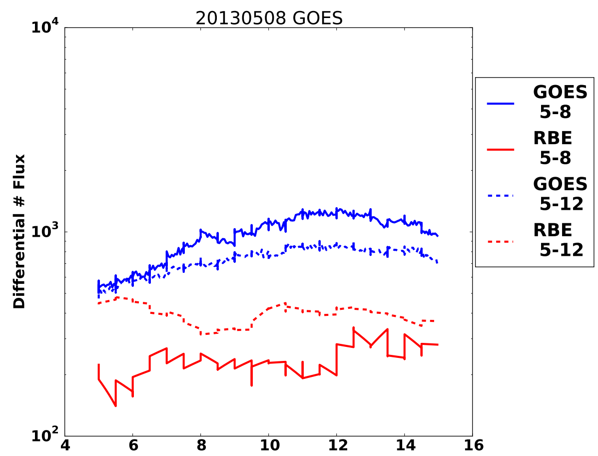

Figure 9: A comparison of GOES-15 2+ MeV electron flux and RBE 2.3 MeV electron flux from 2013-05-08 (post-injection) and 2013-05-12 (quiet).

The RBE fluxes from Figure 9 are interesting. The RBE post-injection and quiet time days are somewhat close to each other, and the quiet time (2013-05-12) electron fluxes are higher than the post-injection fluxes. Once again, this is the opposite of the GOES-15 electron fluxes, suggesting that RBE might not be capturing the radiation belt recovery from a small injection.

We also explored the almost geomagnetic super-storm on 2015-03-17. Figure 10 shows the ACE data (via the CCMC visualization tools). There was strong negative Bz driving throughout the day on 2015-03-17 with recovery commencing on approximately 2015-03-18. Fortunately, when we requested this run, we had asked for 48 hours in order to capture both the main phase of the storm and the recovery period. Thus, we have a wider time span (from 14:00 UT on 2015-03-17 to 23:59 UT on 2015-03-18) to compare GOES-15 and RBE electron fluxes.

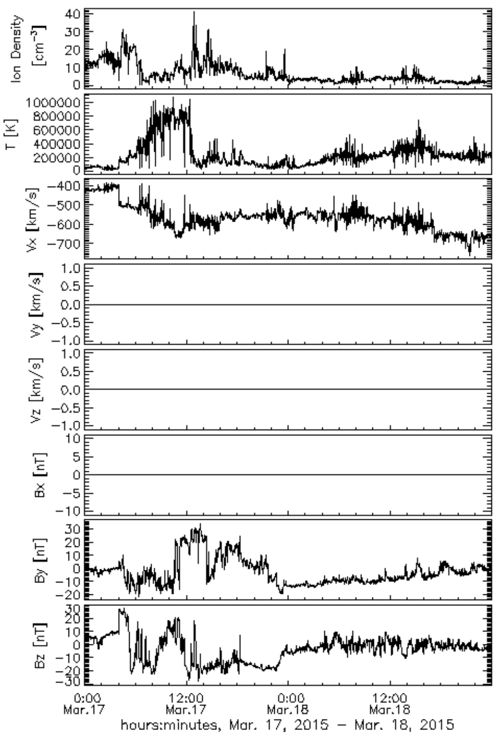

Figure 10: ACE data provided through CCMC for 2015-03-17.

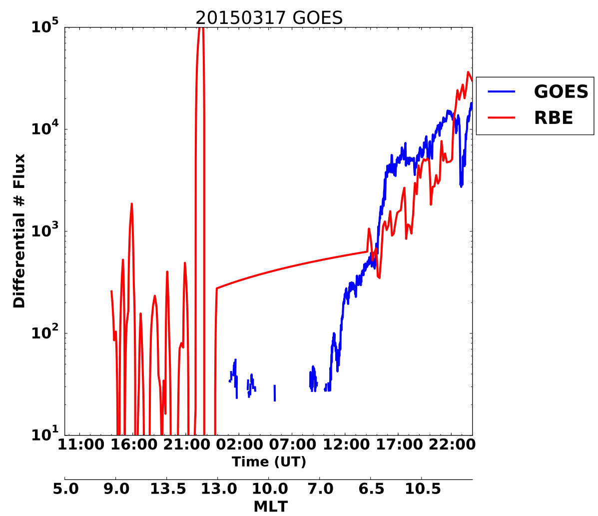

Figure 11: A comparison of GOES-15 2+ MeV electron flux and RBE 2.3 MeV electron flux from 2015-03-17 to 2015-03-18 during an intense geomagnetic storm.

Figure 11 demonstrates RBE's ability to capture the recovery phase of a massive storm well. Although both the model and the data provided patchy data during and immediately after the storm (14 UT on 2015-03-17 to 12 UT on 2015-03-18), the model and data showed similar growth and recovery between 12 UT and 23:59 UT on 2015-03-18. RBE misses a major plunge in electron fluxes seen by GOES-15 at 23 UT, but overall RBE captures the generally behavior of the electron outer radiation belt during recovery.

Analysis

Overall from Figure 8 and Figure 9, there are four things that stand out. The first that RBE is much lower than observed fluxes except during injection times. We expect RBE to provide lower electron fluxes because it is only calculating fluxes for 2.3 MeV whereas GOES-15 is measuring all electron fluxes greater than 2 MeV. However, the RBE rise during storm time relative to GOES-15 measurements suggests that RBE might be overestimating electron fluxes during injections.

The second feature of note is that RBE is missing the noon peak. Electron fluxes in the outer radiation belt peak around MLT = 12 due to solar wind compression of the magnetosphere. The MeV radiation belt electrons should see this peak, as seen in the GOES-15 data. RBE modeled electron fluxes do not show the same relative peak at noon; however, this might be more of a function of the amount of pre-run time for RBE necessary to get a good result. As aforementioned, we found at approximately 14 hours of pre-run, RBE electron fluxes assumed a reasonable distribution with a peak at noon. However, the results may be better if we let RBE pre-run for 24 hours before our intended time period. Further is testing is required before we can assess what is happening here.

The third main feature is that RBE is not showing the same injection recovery process as the GOES-15 data. The GOES-15 data is at a minimum on the injection day, reaches a maximum the day after the injection, and then returns to more normal levels on the quiet day in our May case studies. RBE has a maximum on the injection day, a minimum the day after the injection, and in between electron flux values on the quiet day. This result shows us that RBE is not capturing the entirety of the source/loss processes in this particular injection/series of injections on 2013-05-07.

Dovetailing the first and third feature, we realize that RBE is overestimating injection time fluxes but then these flux values plummet rapidly compared to GOES-15 as RBE electron fluxes recover. So instead of a fresh source of electrons, perhaps accelerated from the ring current, RBE physics suggests that there is increased scattering or a slow loss process involved with recovery. We can rule out magnetopause shadowing where the magnetopause encroaches on the electron radiation belts, allowing some of the electrons to escape on open drift paths because of time scales of magnetopause shadowing. Magnetopause shadowing, which occurs during strong solar wind driving, could be responsible for the injection day minimum seen in GOES-15 data, but it is unlikely to be the cause of loss the day after an injection during a quiet geomagnetic period.

Lastly, our data-model comparison on 2015-03-17 shows that RBE is capturing the dramatic recovery from an intense geomagnetic storm well. Whereas our quiet-time fluxes hover at 10^3 cm^{-2} s^{-1} sr^{-1}, the electron fluxes climb to above 10^4 cm^{-2} s^{-1} sr^{-1}. RBE, although not exact, matches the GOES electron flux measurements well from 12 UT on 2015-03-18 to 23:59 UT on 2015-03-18. There is slight underestimation from 14 UT to 22 UT, but we expect RBE fluxes to be lower because of the 2+ MeV to 2.3 MeV difference. Overall, RBE does a great job of capturing the recovery of an intense geomagnetic storm, which suggests RBE is capturing convection well.

Conclusions

As we improve our radiation belt models, it is crucial to compare with data in order to verify our understanding of the physics of the radiation belts. Using GOES-15 2+ MeV electron fluxes to compare with RBE 2.3 MeV electron fluxes presented many challenges, including determining how many hours of run time is required before RBE reaches steady-state and finding times where there was both model and data available. Unfortunately we were unable to complete the initial goal of this project, which was to determine an offset between RBE and GOES-15 data in order to make a fair comparison and then to test how well RBE faired at capturing storms/injections.

Instead, we focused on determining how long RBE must be run before the output is safely out of the default state (a large post-midnight injection). We found that 14 hours, based on the runs we had available, was sufficient for clearing the default state in RBE. This allowed us to use 10 hours of RBE data from our 2013-05-07, 2013-05-08, and 2013-05-12 and 34 hours of RBE in the 2015-03-17 storm.

In these comparisons, we found that RBE electron fluxes were not capturing the general behavior of GOES-15 electron fluxes. Most notably were in the post-injection recovery period and the expected MLT=12 peak in the electron radiation belts. Figure 8 shows how RBE underestimated the post-injection period and overestimated the injection period electron fluxes. Also, all the May 2013 dates showed that RBE neglected the rise of electron fluxes at noon during this time period.

However, RBE does perform well at capturing electron flux recovery after an intense geomagnetic storm. Figure 11 shows how both model and data fail to capture the behavior of the outer radiation belt during the storm (UT 5:00 on 2015-03-17); however, RBE tracks GOES well as the electron fluxes rise to all time high values post-storm. Our results suggest that RBE is best at modeling intense storm effects compared to injections and quiet time.

For future work, we intend to rigorously determine time scales necessary for RBE to be in a useful steady state and then directly compare RBE to GOES-15 data using a skill score approach.

References

[1] RB Horne, SA Glauert, NP Meredith, D Boscher, V Maget, D Heynderickx, and D Pitchford. Space weather impacts on satellites and forecasting the earth's electron radiation belts with spacecast. *Space Weather*, 11(4):169–186, 2013.

[2] W Lohmeyer, Kerri Cahoy, and Daniel N Baker. Correlation of geo communication satellite anomalies and space weather phenomena: improved satellite performance and risk mitigation. In *30th AIAA International Communications Satellite Systems Conference(ICSSC), Ottawa, Canada*, 2012.

[3] Mei-Ching Fok, Richard B Horne, Nigel P Meredith, and Sarah A Glauert. Radiation belt environment model: Application to space weather nowcasting. *Journal of Geophysical Research: Space Physics (1978–2012)*, 113(A3), 2008.

[4] M-C Fok, A Glocer, Q Zheng, Richard B Horne, Nigel P Meredith, JM Albert, and T Nagai. Recent developments in the radiation belt environment model. *Journal of Atmospheric and Solar-Terrestrial Physics*, 73(11):1435–1443, 2011.

[5] Sarah A Glauert and Richard B Horne. Calculation of pitch angle and energy diffusion coefficients with the padie code. *Journal of Geophysical Research: Space Physics (1978–2012)*, 110(A4), 2005.

[6] A Glocer, G Toth, M Fok, T Gombosi, and M Liemohn. Integration of the radiation belt environment model into the space weather modeling framework. *Journal of Atmospheric and Solar-Terrestrial Physics*, 71(16):1653–1663, 2009.

[7] Daniel N Baker, Glenn M Mason, Orlando Figueroa, G Colon, JG Watzin, and Roberto M Aleman. An overview of the solar anomalous, and magnetospheric particle explorer (sampex) mission. *Geoscience and Remote Sensing, IEEE Transactions on*, 31(3):531–541, 1993.

[8] DN Baker, SG Kanekal, VC Hoxie, S Batiste, M Bolton, X Li, SR Elkington, S Monk, R Reukauf, S Steg, et al. The relativistic electron-proton telescope (rept) instrument on board the radiation belt storm probes (rbsp) spacecraft: Characterization of earths radiation belt high-energy particle populations. In *The Van Allen Probes Mission*, pages 337–381. Springer, 2014.

[9] JV Rodriguez, TG Onsager, and JE Mazur. The east-west effect in solar proton flux measurements in geostationary orbit: A new goes capability. *Geophysical Research Letters*, 37(7), 2010.

[10] T Neil Davis and Masahisa Sugiura. Auroral electrojet activity index ae and its universal time variations. *Journal of Geophysical Research*, 71(3):785–801, 1966.